Evaluation of the systematic shifts of a single-$^{40}Ca^{+}$-ion frequency standard

Yao Huang,[1,2,4] Qu Liu,[1,2,4] Jian Cao,[1,2,4] Baoquan Ou,[1,2,*] Peiliang Liu,[1,2,4] Hua Guan,[1,2,3] Xueren Huang,[1,2,3] and Kelin Gao[1,2,3,†]

[1]*State Key Laboratory of Magnetic Resonance and Atomic and Molecular Physics, Wuhan Institute of Physics and Mathematics, Chinese Academy of Sciences, Wuhan 430071, China*

[2]*Key Laboratory of Atomic Frequency Standards, Wuhan Institute of Physics and Mathematics, Chinese Academy of Sciences, Wuhan 430071, China*

[3]*Center for Cold Atom Physics, Chinese Academy of Sciences, Wuhan 430071, China*

[4]*Graduate School, Chinese Academy of Sciences, Beijing 100080, China*

(Received 13 April 2011; published 21 November 2011; corrected 19 January 2012)

Progress on the evaluation of systematic frequency shifts is described in the development of the optical frequency standard based on single-trapped $^{40}Ca^{+}$ with a "clock" transition at 729 nm. The overall systematic uncertainty of the $4s\ ^2S_{1/2}$-$3d\ ^2D_{5/2}$ clock resonance has been characterized to be 7.8×10^{-16}. This uncertainty is at a level similar to the Cs fountain primary standard, while the potential stability for the $^{40}Ca^{+}$ clock exceeds that of Cs.

DOI: 10.1103/PhysRevA.84.053841 PACS number(s): 42.62.Fi, 06.30.Ft, 37.10.Ty

I. INTRODUCTION

Optical frequency standards have recently been significantly developed thanks to the invention of optical frequency comb technology [1] and ultranarrow-linewidth lasers. The optical transitions have large line quality factors (Q) [2,3], thus optical frequency standards based on optical transitions are expected to replace the microwave standard in Cs, as in the definition of the SI second, in the near future. Recently, the optical clock based on a single trapped Hg^{+} ion has surpassed Cs fountain clocks [4,5] in terms of accuracy, with clock systematic uncertainty reduced to 7×10^{-17} [6]. At the same time, the uncertainty of a Sr optical lattice clock has reached the 1×10^{-16} fractional level [7] and the Yb optical lattice clock just reached 3.4×10^{-16} [8]. The best evaluation of the frequency inaccuracy reported so far would be $\sim 8.6 \times 10^{-18}$ with Al^{+} [9]. Other high-accuracy optical standards based on a single ion have been developed, with an inaccuracy on the order of 10^{-15} in Sr^{+} [10], Yb^{+} [11], and Ca^{+} [12]. The inaccuracy of the standards above is mainly limited by the electric quadrupole shift, the ac Stark shift, and the blackbody radiation shift.

A single Ca^{+} ion has been proposed to be one of the candidates for the future frequency standards [13,14]. An optical frequency standard based on Ca^{+} is being developed by the Quantum Optics and Spectroscopy Group in Innsbruck, Austria, the National Institute of Information and Communications in Japan (NICT), and University of Provence in France. In Innsbruck, the ion is trapped in a linear Paul trap and cooled by both Doppler cooling and sideband cooling. A magnetic field of 3.087(2) G is used to split the Zeeman transitions. The uncertainty of the absolute frequency measurement was evaluated to be 2.4×10^{-15} referenced to the transportable Cs atomic fountain clock of LNE-SYRTE [12] and a measurement with a 10^{-14} uncertainty level was reported with the Paul trap and Doppler cooling by NICT [15].

In this paper, we report a detailed study of the systematic uncertainty with the $^{40}Ca^{+}$ $4s\ ^2S_{1/2}$-$3d\ ^2D_{5/2}$ transition frequency of 7.8×10^{-16}. This result shows that the $^{40}Ca^{+}$ optical clock can reach an uncertainty level close to Cs fountains, while the potential stability for the system is far greater. Meanwhile, an Allan deviation of below the 10^{-14} level at 10 000 s is obtained from the comparison between the $^{40}Ca^{+}$ optical frequency standard and a H maser using a femtosecond laser frequency comb.

II. EXPERIMENTAL SETUP

The $^{40}Ca^{+}$ has a simple energy-level scheme (Fig. 1) which has good potential accuracy and low systematic shifts. The "clock" transition is the electric quadrupole $4s\ ^2S_{1/2}$-$3d\ ^2D_{5/2}$ transition at 729 nm, which has a natural linewidth of 0.2 Hz [16]. Full details of the laser cooling, trapping detecting, and probing system used in this work are reported in previous works [17,18]. Briefly, loaded by ionizing at a neutral Ca atom beam with electron bombardment, a single ion of $^{40}Ca^{+}$ is trapped and cooled in a miniature Paul ring trap with two endcaps and one ring, with an endcap-to-center distance of $z_0 \approx 0.7$ mm and a center-to-ring electrode distance of $r_0 \approx 0.8$ mm. Two other electrodes perpendicular to each other are set in the ring plane to compensate for the ion's excess micromotion. A trapping rf of 630 V_{p-p} is applied to the ring at a frequency of 9.8 MHz. Based on measurements of the ion motion sideband spectra, the secular frequencies of the trap were to be $\omega_x \approx \omega_y \approx 700$ kHz and $\omega_z \approx 1.5$ MHz, respectively. Typically, $\sim 10\ \mu$W of the 397-nm laser power is focused on the single ion with a spot size of $\sim 40\ \mu$m, 600 μW of power with 60 μm size for the 866-nm laser, 150 μW of power with 60 μm size for the 854-nm laser, and 40 nW of power with 100 μm size for the 729-nm laser, respectively. Both the 397- and 866-nm lasers are stabilized to the 729-nm laser using transfer cavities. The clock laser at 729 nm is locked to a high-finesse cavity (Zerodur material) using the Pound-Drever-Hall technique [19]. A typical linewidth (FWHM) of 20 Hz was measured from the heterodyne beat note with another laser system at a time scale of ~ 300 ms. The long-term drift of the laser is measured to be ~ 3 Hz/s,

*Permanent address: Department of Physics, National University of Defense Technology, Changsha, 410073, China.

†klgao@wipm.ac.cn

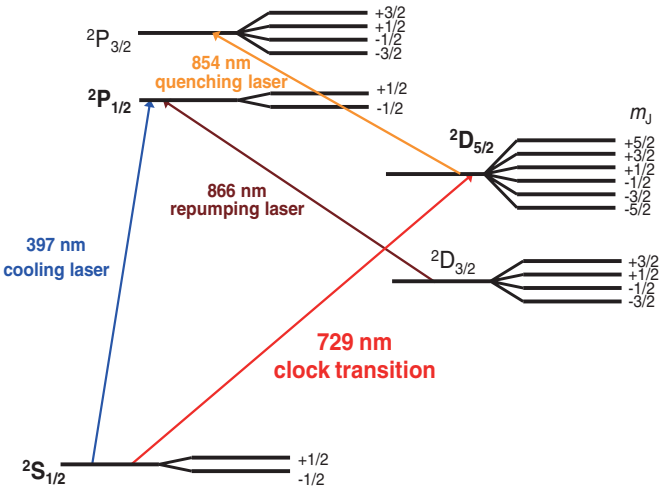

FIG. 1. (Color online) Partial energy-level diagram of $^{40}Ca^+$ showing the principal transitions used in cooling, repumping, and probing of the reference 729-nm transition.

indicated both by the comb measurements and the observation of the ion transitions.

The clock transition is observed by the electron-shelving method [20]. A pulse-light sequence is introduced to observe the clock transition spectrum in order to avoid ac Stark shift caused by the 397-, 866-, and 854-nm radiations. The 729-nm radiation is incident for ∼10 ms, which induces a Fourier limited linewidth of ∼100 Hz, while the other radiations are blocked. Then the state of the ion is interrogated using the cooling lasers. If the count rate is smaller than a fixed threshold, the clock transition has taken place. After that, the ion is initialized again using the 854-nm radiation. The 729-nm laser is locked to the clock transition by the "four points locking scheme" [21,22] using a double-passed acousto-optic modulator (AOM) which shifts the laser frequency to match the transition [23]. The required AOM frequencies are updated every 40 cycles of pulses, which takes ∼1.5 s. The 729-nm laser is locked to six chosen Zeeman transitions to do the measurements: $M_J = \pm 1/2$, $M_J = \pm 3/2$ and $M_J = \pm 5/2$ for the $D_{5/2}$ level one after another to null the electric quadrupole shift, i.e., the laser is locked to the innermost components, the second innermost components, and then the inner pair of $\Delta M_J = \pm 2$ components; each pair takes 6 s. The probe laser frequency is measured by averaging sets of the comb frequency readings of the beat note of the mode-locked fs laser and the probe laser every 1 s. Both the repetition frequency and the offset frequency of the comb (FC8004, MenloSystems) are locked to two individual synthesizers, which are referenced to a 10 MHz signal provided by an active hydrogen maser (CH1-75A).

The excess micromotion is minimized before each measurement with the observation by the rf-photon correlation method [24] by adjusting the endcap and compensation electrode voltages. After the optimization of the electrode voltages, the ion can stay in the trap without any laser for up to 30 h. Double-layer magnetic shields have been mounted around the ion trap vacuum chamber, and a shielding factor of ∼1/200 is measured in a dc magnetic field of ∼1 G. A dc magnetic field of ∼430 nT is applied after compensating the residual field in the trap by three pairs of coils perpendicular to each other with three individual current sources. With this small magnetic field, the splitting for ten Zeeman transitions is ∼35 kHz [Fig. 2(a)]. An electro-optic modulator (EOM) is used for modulating the polarization of the repumping laser with frequency ∼10 MHz to avoid the Hanle effect. One of the $\Delta M_J = 0$ components is observed to be ∼100 Hz linewidth with a Lorentzian fit [Fig. 2(b)].

III. ESTIMATION OF THE CLOCK TRANSITION SHIFTS

There are a variety of potential sources of systematic shift which might be associated with the quadrupole 729-nm $4s\ ^2S_{1/2}$-$3d\ ^2D_{5/2}$ clock transition in a laser-cooled trapped $^{40}Ca^+$ ion as follows.

The second-order Doppler shift is caused by the relativistic Doppler effect, due to the ion motion relative to the laboratory frame, with either the thermal kinetic energy or the micromotion. For our ring trap, after the minimization of the micromotion, the ion temperature is estimated from the intensity of the secular sidebands relative to the carrier (normally ∼0.3–0.8), yielding a mean temperature of 4(2) mK [25]. With the ion temperature estimated, the second Doppler shift caused by thermal kinetic energy is calculated to be –0.006(0.003) Hz [26]. As for the second Doppler shift

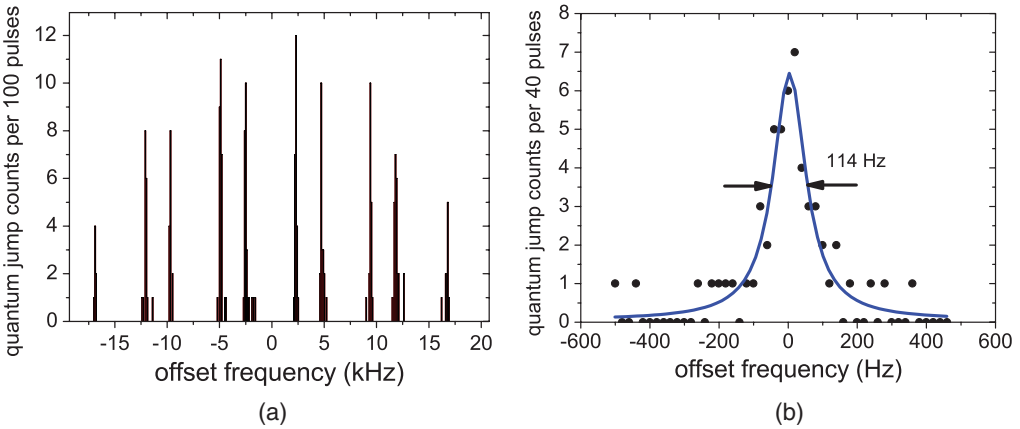

FIG. 2. (Color online) (a) Ten components of the Zeeman profile $4s\ ^2S_{1/2}$-$3d\ ^2D_{5/2}$ clock transition with the whole separation of 34 kHz in the magnetic field of ∼0.43 μT; (b) one of the $\Delta M_J = 0$ components which was achieved with the 729-nm scanning step of 6 Hz; the fitted curve is the Lorentzian fit and yields a linewidth of 114(11) Hz.

caused by micromotion, it can be estimated by observing the intensity of the micromotion sidebands relative to the carrier or observing the cross-correlation signal [24]. From the correlation signal observed, typically with a modulation amplitude ratio of 0.2(0.1), and considering the direction of the micromotion is not well known, the shift is estimated to be –0.02(0.02) Hz.

Thermal secular motion and excess micromotion can push the ion into nonzero mean-square electric fields from the trap, which introduce a Stark shift. The Stark shift due to micromotion can be calculated from the ion temperature above that for the three pair of transitions [24,27,28]; our total averaged Stark shift due to micromotion should be <1 mHz. For the Stark shift due to thermal motion, for the three pairs of components as above, we can calculate the total average shift is also <1 mHz from the correlation signal [26,28]. There is also a Stark shift arising from blackbody radiation. At a room temperature of 293 K, assuming the real temperature fluctuation would be 2 K, the shift would be 0.35(0.02) Hz [28].

The radiation used to cool and probe the trapped ion can cause ac Stark shifts of the clock transition frequency. For the 397-nm laser, a shutter and an AOM are used to switch off the laser beam. The frequency difference between the states with AOM always on and with AOM off when doing the interrogations with the 729-nm laser is measured to be <10 Hz. Therefore, with an attenuation of better than 40 dB for the AOM which switches off the 397-nm radiation when the measurements are made, the shift is <1 mHz. For the laser at 866 nm, a shutter is used to switch off the light; the frequency difference of <30 Hz between having the shutter always on and having it off when doing the interrogations with the 729-nm laser was measured. Therefore, with an attenuation of better than 70 dB for the shutter which switches off the 866-nm radiation when the measurements are made, the shift is <1 mHz. For the 854-nm laser beam, two individual shutters are used to block the light. The frequency difference between having the 854-nm laser off and having only one shutter off when doing the interrogations with 729-nm laser is measured to be <20 Hz. Therefore, with an attenuation of better than 70 dB for the other shutter which switches off the 854-nm radiation when the measurements are made, the shift should be <1 mHz. The ac Stark shift caused by the 729-nm laser is measured by doing measurements at different probe laser intensities. From the experiment results, we obtain a linear fit slope of 0.04(0.06) Hz/I_0, where I_0 is the typical intensity we used for measurements.

The linear Zeeman effect can be effectively canceled out by locking to a pair of Zeeman components which are symmetrically placed around the line center. However, there may be ac broadening of the components and the fast changes of the dc magnetic field could cause a locking problem. As for the long-term dc magnetic field drift as well as the probe laser cavity drift, we can estimate the shifts using the servo error signal. In our case, the servo error would be 0.11(0.03) Hz. Slower field drift, especially from 0.05 to 0.2 Hz, could cause a linear Zeeman shift. We measured the slow magnetic field drift, mainly slower than 0.3 Hz. From the measurement of the different Zeeman components, which split proportional to the field, we can evaluate the stability of the field. From the calculation, the statistical error of the linear Zeeman shift was 0.24 Hz. As for the second-order Zeeman shift, it can be calculated using second-order perturbation theory [29]. For our system, the average magnetic field during the measurements is 430 nT and the fluctuation of the field we measured is ~3 nT. This leads to a second Zeeman shift of <1 mHz, which is negligible.

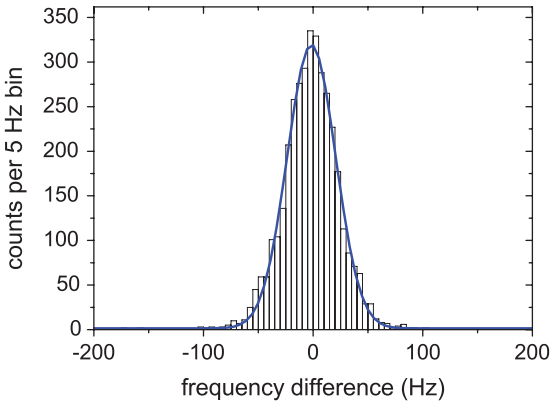

FIG. 3. (Color online) A histogram of the measurement frequency data of the center frequency difference for the $M_J = \pm 1/2$ and $M_J = \pm 3/2$ components. The blue line shows a Gaussian fit of 44.2(0.5) Hz standard deviation. The error for the center is 0.23 Hz.

The largest source of systematic frequency shift for the optical frequency standard arises from the electric quadrupole shift of the reference transition [30] due to the presence of electric field gradients, which interact with the electric quadrupole moment of the ion. However, the quadrupole shift can be nulled by using several techniques, and the uncertainty in this shift can be reduced to a substantially lower level. The clock laser is locked to the six different chosen Zeeman transitions one after another. By averaging the center frequency of the three pairs of the components, we can null the quadrupole shift [9]. According to the magnetic field drift rate we measured, normally <1 nT per hour, the 6 s of

TABLE I. The systematic frequency shifts and their associated errors in Hz; the fractional uncertainty is in units of 10^{-15}.

Effect	Shift (Hz)	Error (Hz)	Fractional error ($\times 10^{-15}$)
Second-order Doppler shift due to thermal motion	–0.006	0.003	0.01
Second-order Doppler shift due to micromotion	–0.02	0.02	0.05
Stark shift due to thermal motion	0	<0.001	<0.001
Stark shift due to micromotion	0	<0.001	<0.001
ac Stark shift due to 397 nm	0	<0.001	<0.001
ac Stark shift due to 866 nm	0	<0.001	<0.001
ac Stark shift due to 854 nm	0	<0.001	<0.001
ac Stark shift due to 729 nm	0.04	0.06	0.15
Blackbody radiation shift	0.35	0.02	0.05
Servo error and shift	0.11	0.03	0.07
Linear Zeeman shift	0	0.24	0.58
Second-order Zeeman shift	0	<0.001	<0.001
Electric quadrupole shift	0	0.21	0.51
Total shift	0.47	0.32	0.78

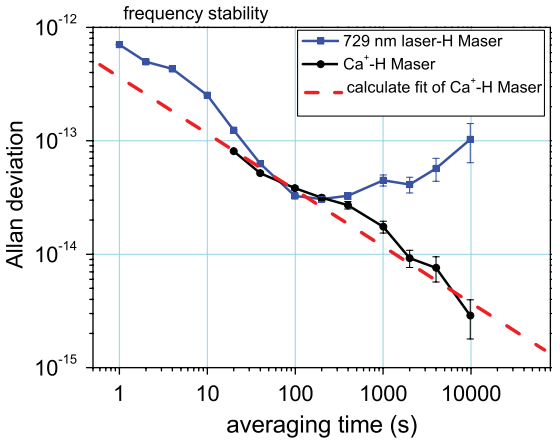

FIG. 4. (Color online) Allan deviations of both the comparison instabilities of the probe laser vs the H maser (black line and symbol) and the $^{40}Ca^{+}$ optical clock vs the H maser (blue line and symbol).

measuring time difference can induce a shift error of <0.02 Hz. By averaging the difference of center frequency for different components, an error of 0.23 Hz was obtained (Fig. 3).

Table I shows the total summary of the frequency shifts considered above. Considering all of them, we get a total shift of 0.47 Hz with an error of 0.32 Hz, which is 7.8×10^{-16} of a fractional error.

IV. ESTIMATION OF THE FREQUENCY STABILITY

Frequency instability comparison for both the probe laser vs the H maser and the $^{40}Ca^{+}$ optical clock vs the H maser are obtained with 40 h of measurements, and the Allan deviation is calculated. As shown in Fig. 4, the Allan deviation for the ion is much better than the probe laser, and goes below the 10^{-14} level at 10 000 s. A fit with $\tau^{-1/2}$ is also shown in the figure; we calculated the trend of the Allan deviation would be $3.71(0.15) \times 10^{-13} \times \tau^{-1/2}$.

V. CONCLUSION

From the systematic shift errors considered above, it appears that detailed experiments with $^{40}Ca^{+}$ optical frequency could lead to an uncertainty of better than 10^{-16}. The electric quadrupole shift and the ac Stark shift due to 729-nm laser are dominating the uncertainty budget. The uncertainty of the electric quadrupole shift is large, mainly due to the large statistical error, which is caused by the servo system not being fast enough to follow the ion transition induced by the nonlinear drift of the probe laser and the instability of the dc magnetic field. The $^{40}Ca^{+}$ optical clock vs H maser comparison instability was limited by the stability of the H maser and the transfer cable noise. Our probe laser needs to be improved, especially on the nonlinear drift and the linewidth, which could be done by improving the environment: both the stability of the room temperature and the vibration control. We plan to set up another $^{40}Ca^{+}$ optical clock to do the comparison of the two traps to achieve a better Allan deviation. In the near future we will calibrate the H maser with Cs fountain clock for the measurement of the absolute frequency of the $4s\ ^2S_{1/2}$-$3d\ ^2D_{5/2}$ transition.

ACKNOWLEDGMENTS

We gratefully acknowledge H. Shu, H. Fan, B. Guo, and W. Qu for the early works. We also thank G. Huang and J. Li for help and working with us. We thank J. Ye, J. Bergquist, K. Matsubara, Y. Li, and L. Ma for help and fruitful discussions. We thank M. Chwalla for discussion on the evaluation of the quadrupole shift error. We thank H. Klein for fruitful discussions and a critical reading of the manuscript. This work is supported by the National Basic Research Program of China (2005CB724502), the National Natural Science Foundation of China (Grants No. 10874205, No. 10774161, and No. 11034009) and the Chinese Academy of Sciences.

[1] T. Udem *et al.*, Nature **416**, 233 (2002).
[2] M. M. Boyd *et al.*, Science **314**, 1430 (2006).
[3] R. J. Rafac, B. C. Young, J. A. Beall, W. M. Itano, D. J. Wineland, and J. C. Bergquist, Phys. Rev. Lett. **85**, 2462 (2000).
[4] S. Bize *et al.*, J. Phys. B **38**, S449 (2005).
[5] T. P. Heavner *et al.*, Metrologia **42**, 411 (2005).
[6] W. H. Oskay *et al.*, Phys. Rev. Lett. **97**, 020801 (2006).
[7] A. D. Ludlow *et al.*, Science **319**, 1805 (2008).
[8] N. D. Lemke, A. D. Ludlow, Z. W. Barber, T. M. Fortier, S. A. Diddams, Y. Jiang, S. R. Jefferts, T. P. Heavner, T. E. Parker, and C. W. Oates, Phys. Rev. Lett. **103**, 063001 (2009).
[9] C. W. Chou, D. B. Hume, J. C. J. Koelemeij, D. J. Wineland, and T. Rosenband, Phys. Rev. Lett. **104**, 070802 (2010).
[10] H. S. Margolis *et al.*, Science **306**, 1355 (2004).
[11] T. Schneider, E. Peik, and C. Tamm, Phys. Rev. Lett. **94**, 230801 (2005).
[12] M. Chwalla *et al.*, Phys. Rev. Lett. **102**, 023002 (2009).
[13] C. Champenois *et al.*, Phys. Lett. A **331**, 298 (2004).
[14] M. Kajita, Y. Li, K. Matsubara, K. Hayasaka, and M. Hosokawa, Phys. Rev. A **72**, 043404 (2005).
[15] K. Matsubara *et al.*, Appl. Phys. Express **1**, 067011 (2008).
[16] P. A. Barton, C. J. S. Donald, D. M. Lucas, D. A. Stevens, A. M. Steane, and D. N. Stacey, Phys. Rev. A **62**, 032503 (2000).
[17] H. L. Shu *et al.*, Chin. Phys. Lett. **22**, 1641 (2005).
[18] H. L. Shu *et al.*, Chin. Phys. Lett. **24**, 1217 (2007).
[19] H. Guan *et al.*, Opt. Commum. **284**, 217 (2011).
[20] H. Dehmelt, IEEE Trans. Instrum. Meas. **31**, 83 (1982).
[21] J. E. Bernard, A. A. Madej, L. Marmet, B. G. Whitford, K. J. Siemsen, and S. Cundy, Phys. Rev. Lett. **82**, 3228 (1999).
[22] G. Barwood *et al.*, IEEE Trans. Instrum. Meas. **50**, 543 (2001).
[23] Q. Liu *et al.*, Chin. Phys. Lett. **28**, 013201 (2011).
[24] D. J. Berkeland *et al.*, J. Appl. Phys. **83**, 5025 (1998).
[25] S. Urabe *et al.*, Appl. Phys. B: Lasers Opt. **67**, 223 (1998).
[26] A. A. Madej, J. E. Bernard, P. Dube, L. Marmet, and R. S. Windeler, Phys. Rev. A **70**, 012507 (2004).
[27] J. R. P. Angel and P. G. H. Sandars, Proc. R. Soc. London Ser. A **305**, 125 (1968).
[28] B. Arora, M. S. Safronova, and C. W. Clark, Phys. Rev. A **76**, 064501 (2007).
[29] E. E. Anderson, *Modern Physics and Quantum Mechanics* (Saunders, Philadelphia, PA, 1971), p. 288.
[30] G. P. Barwood, H. S. Margolis, G. Huang, P. Gill, and H. A. Klein, Phys. Rev. Lett. **93**, 133001 (2004).